Materials Research Bulletin 49 (2014) 35–38

Contents lists available at ScienceDirect

Materials Research Bulletin

journal homepage: www.elsevier.com/locate/matresbu

Short communication

Study the gas sensing properties of boron nitride nanosheets

Muhammad Sajjad, Peter Feng *

Department of Physics, University of Puerto Rico, P.O. Box 70377, San Juan 00925, Puerto Rico

ARTICLE INFO

Article history:
Received 5 December 2012
Received in revised form 11 August 2013
Accepted 16 August 2013
Available online 28 August 2013

Keywords:
A. Multilayers
B. Laser deposition
C. Electron microscopy
C. Raman spectroscopy
D. Crystal structure

ABSTRACT

In the present communication, we report on the synthesis of boron nitride nanosheets (BNNSs) and study of their gas sensing properties. BNNSs are synthesized by irradiating pyrolytic hexagonal boron nitride (*h*-BN) target using CO_2 laser pulses. High resolution transmission electron microscopic measurements (HRTEM) revealed 2-dientional honeycomb crystal lattice structure of BNNSs. HRTEM, electron diffraction, XRD and Raman scattering measurements clearly identified *h*-BN. Gas sensing properties of synthesized BNNSs were analyzed with prototype gas sensor using methane as working gas. A systematic response curve of the sensor is recorded in each cycle of gas "in" and "out"; suggesting excellent sensitivity and high performance of BNNSs-based gas-sensor.

1. Introduction

The development of gas-sensor devices with optimized sensitivity has been gaining prominence interest in material technology. The use of a semiconductor fabrication line is a preferred manufacturing process because of the potential to reduce cost. However, fundamental materials and processing issues which are critical for a high-performance gas sensor operating in harsh environment, need to be addressed. Recently, graphene-based gas-sensors has been fabricated and tested [1]. The successful implementation of graphene as a gas sensor has brought interest toward other ultra-thin nanomaterials such as boron nitride nanosheets (BNNSs) [2–5]. Nanocrystalline boron nitride (BN) offers immence promise for improve senstivity of the sensor for different working gasses. Previously, the gas sensing properties of boron nitride nanotubes (BNNTs), and C-doped BNNTs for various gases, such as CH_4, CO_2, H_2, N_2, NO_2, O_2, and F_2, have been investigated by using the density functional theory calculations [6–10]. Due to the small surafce area, BNNTs are found less sensitive to various gaseous molecules. On the other hand, few atomic layers BNNSs are fascinating for high-performance gas-sensors. Within the layers of BNNSs, the chemical alternation of boron (B) and nitrogen (N) atoms cause the ionic nature of this crystal that could be highly sensitive to various gasses. The electronic properties of BNNSs are largely change by the adsorption of gas molecules, which is a prerequisite for gas-sensor. Moreover, the two-dimensional nature of BNNSs allows a total exposure of all its atoms to the adsorbing gas molecules which increases the sensitivity of sensor. Because of high thermal stability and chemical inertness, this material can also be used in harsh environment where other materials cannot be used.

Several methods have been proposed to prepare BNNSs, including decomposition of borazine, ultrasonification processing of *h*-BN, peeling by scotch adhessive tapes, and chemical exfoliations of *h*-BN in ways similar to graphene fabrication [6,8,11]. These approaches represent a significant step toward synthesis of nanosheets. However, these techniques require high temperature high pressure (HTHP), and sometimes catalyst for the scale production of the material [12]. The requirements of HPHT conditions assisted with various catalysts limits to incorporate pure BNNSs for practical applications. So far, it was a challenge to prepare pure BNNSs for the fabrication of a resistance-based gas sensor. In this paper, we report on the synthesis of high quality BNNSs on silicon (Si) substrate and their gas sensing properties.

2. Experimental conditions

The nanosheets are synthesized by irradiating a pyrolytic *h*-BN target (2.00″ diameter × 0.125″ thick, 99.99% purity, *B*/*N* ratio ~ 1.05, density ~ 1.94 g/cc) using CO_2-pulsed laser deposition technique (CO_2-PLD: wavelength: 10.6 μm, pulse width: 1–5 μs, repetition rate: 5 Hz, and pulse energy: 5 J). The laser beam focused on to the target with a 30 cm focal length ZnSe lens and

* Corresponding author. Tel.: +1 7877640000x2719.
E-mail address: p.feng@upr.edu (P. Feng).

0025-5408/$ – see front matter © 2013 Elsevier Ltd. All rights reserved.
http://dx.doi.org/10.1016/j.materresbull.2013.08.019

incident angle 45° relative to a rotated (speed of circa 200 rpm) target under high vacuum (2.66×10^{-5} Pa). The power density of the laser on the target was controlled at 2×10^8 W/cm^2 per pulse. A silicon (Si 100) wafer was mounted onto the substrate holder 3 cm away from the target. Prior to deposition, the substrate was rinsed in acetone and methanol in sequence to remove the surface impurities. Substrate temperature (400 °C) was controlled by using a thermocouple and a heater. The deposition time was kept 8 min.

Gas sensing properties of BNNSs were studied in a home-made gas-sensor devise. The detail related to device can be found out in our previous publications [13,14]. BNNSs/Si substrate was connected to a precise resistor and a battery to form a voltage–current–resistor (*V–I–R*) electrical circuit as a prototype sensor. Sensitive characters of BNNSs-based sensor were examined based on the measurement of the voltage drop across the precise resistor so that the variation of the electrical conductivity of the sensor can be estimated.

3. Results and discussion

Scanning electron microscopic (SEM) image (Fig. 1a) shows that the entire substrate surface is covered with BNNSs. Transmission electron microscopic (TEM) measurements (Fig. 1b) identified that BNNSs are mainly consist of many overlapping sheet structures. For further structural characterizations, electron beam is focused on a flat layer of BNNSs. This time we used a high-resolution TEM (HRTEM) equipped with an imaging aberration corrector, operated at 200 kV to directly characterize the crystalline structures of nanosheets. Results are shown in Fig. 1c. It can be found that BNNSs consist of a large amount of highly ordered B and N atoms packed in a honeycomb crystal lattice structure of six-membered B_3–N_3 hexagon. The image (Fig. 1c) does not show atomic defects, though we operate the microscope at 200 keV. We mitigated the appearance of defects due to knock-on damage by examining the materials as quickly as possible with reduced illumination. It is well known that the threshold for B atoms and N atoms in BN nanotubes are around 74 keV and 84 keV, respectively [15]. Fig. 1d shows the experimentally observed selected area electron diffraction (ED) pattern. A series of electron diffraction spots arranged in typical hexagonal pattern confirmed single crystalline structure of synthesized BNNSs.

The formation of BNNSs is based on planer growth stage in which the base layer is flat and parallel to the substrate. The general interpretation of mechanism for the formation of BNNSs is that; when the laser beam impacts the target surface, it generates a plasma plume out of the target surface directed toward the surface of substrates. This plasma plume is composed of high energy boron nitride ions and clusters. When these ions and clusters land onto the substrate surface, the extra thermal activation besides substrate heating provides energy exchange through collisions between active ions, clusters and atoms of BN [12]. This helps to grow small BN layers that coalesce and transform into a uniform BN nanosheet. Further incoming B and N ions and clusters land onto the surface of growing nanosheet would rapidly move along the sheet surface, reach the edge of the nanosheet, and covalently bond with the edge atoms. It is thus appears that during the first few minutes of synthesis, BN layer grows parallel to the substrate surface. After the development of sufficient force onto the grain boundaries, the leading edge of the layer partially curled upward, which is an intrinsic property of 2D crystalline structure or it is due

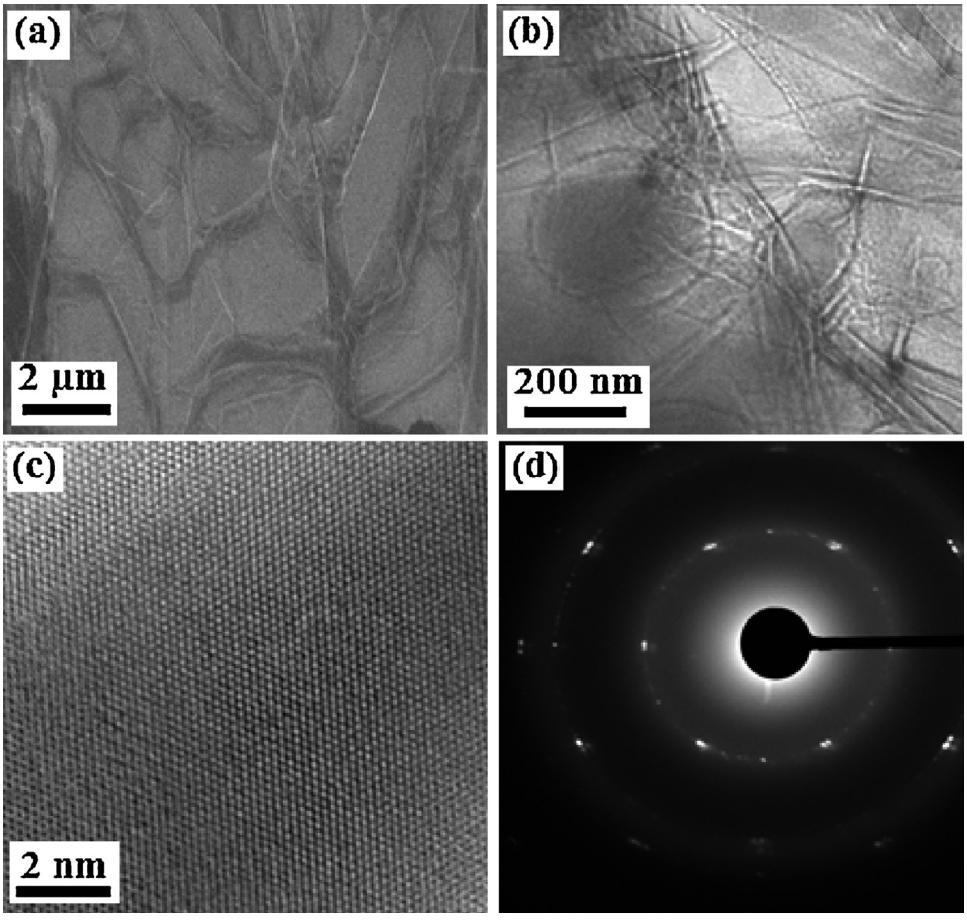

Fig. 1. Microscopic images of BNNSs, (a) SEM, (b) low magnification TEM, (c) HRTEM and (d) ED pattern of BNNSs. The scalar bars are shown on the images.

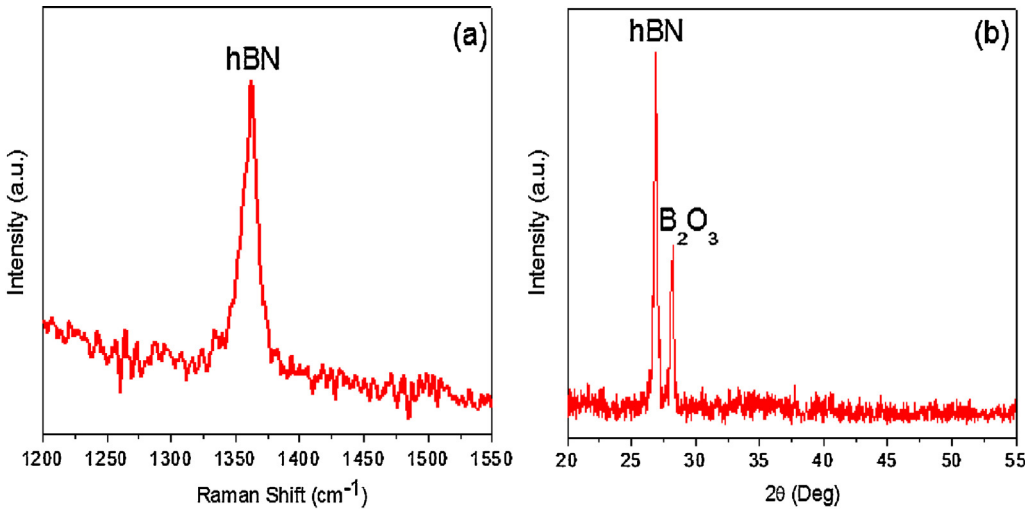

Fig. 2. (a) Raman spectrum and (b) XRD pattern of BNNSs.

to weak van der Wall force that connects deposited layer to the substrate surface. Now, it could be possible that incoming BN species diffuse toward the surface of initially growing layer instead of toward the growing edges. In this process, a second layer starts growing on top of the first layer and so on. This process continues layer by layer and consequently we get a finite BN nanosheet. This mechanism accounts for the observation that rather than forming a continuous BN nanosheet parallel to the substrate, we observe self-assembly of multiple set of BNNSs that are oriented horizontally. A similar mechanism has been proposed for the formation of carbon nanosheets produced by radio frequency plasma enhanced CVD method [16].

The crystalline structure of BNNSs was analyzed by Raman spectroscopy and XRD diffraction pattern. An intense Raman active E_{2g} vibrational mode identified at ~1365 as shown in Fig. 1a is related to hexagonal crystalline structure [17]. Fig. 2(b) shows XRD pattern of BNNSs where a high intensity peak appeared at 2θ ~26.84° is indicating *h*-BN (0 0 2) phase [18]. A small peak appeared at around 28.24° related to B_2O_3 deformation mode [19].

After characterization of the crystalline structure of nanosheets, the BNNSs/Si sample was placed inside the gas-sensor device in order to analyze the gas sensing properties of BNNSs. The operating

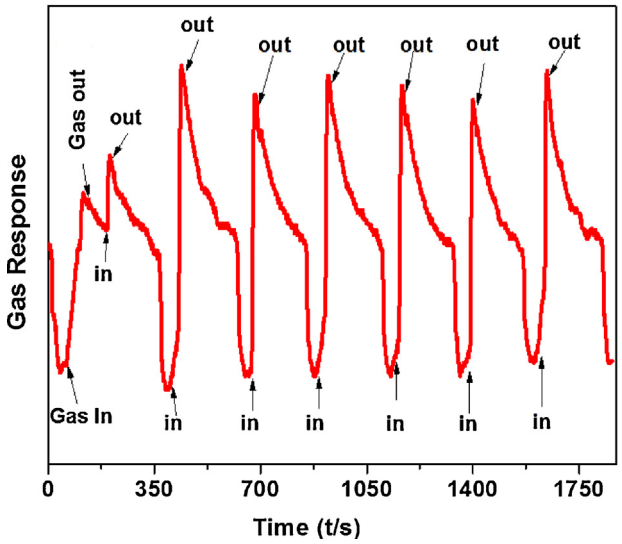

Fig. 3. A typical response curve of BNNSs for CH_4 gas.

temperature of the sensor was fixed at 175 °C. Methane (CH_4) gas was introduced in the chamber in eight cycles and the transient response behavior of the prototypic sensor was recorded for each cycle of gas "in" and "out". The result is presented in Fig. 3. Good repeatability, quick response and recover time of the sensor have been obtained from the characterization. Actually, response time and recover time should be shorter. This is because time delay in switching on or off the valves of gas inlet and outlet, as well as low pumping capacity (7 m^3/h) would affect the measurement results. Unlike zero-bandgap graphene or small bandgap semiconducting single walled nanotubes (SWNTs), BNNSs are wide bandgap semiconductor or a defacto insulator. So it is quite interesting to observe that pure BNNSs can be a good resistance-based gas sensor.

BNNSs based gas-sensors operates by measuring changes in electrical resistance of the surface as it undergoes reduction with the CH_4 gas. Though the exact mechanism is still to be investigated, it appears that at the present working temperatures (175 °C), free electrons can move easily through the surface and across the boundaries between crystal grains of BNNSs. However, when CH_4 is introduced, it is adsorbed on the surfaces and at the grain boundaries of BNNSs, it removes free electrons from the underlying material, creating a potential barrier at the grain boundaries of the nanosheets. Moreover, CH_4 molecules are polarized, they are easier to be absorbed by the surface and grain boundaries of BNNSs and then change the conductivity of the surface [14]. This is manifested as an increase in resistance. It is noticed, in the first two cycles, the response signal of the sensor is poor as shown in Fig. 3. Probably, the possible contamination on the surface of BNNSs affects the sensitivity of the sensor. After the first two cycles, the signal of the sensor quickly increases to its maximum value. This is due to the fact that the impurities present on nanosheets surface might be pumped out with the CH_4 gas. Almost similar trend in the response curve has been found for the next cycles of gas in and out. We repeated this experiment several times and get the same result. The transient response behavior of BNNSs-based gas sensor for various other gasses is under investigation.

4. Conclusions

In summary, atomic layers BNNSs can be synthesized using CO_2-PLD technique. In the form of honeycomb network, the surface chemistry of BNNSs is petty suitable for the possible reaction of

CH_4 gas molecules with B and N atoms, ultimately results in high sensitivity; therefore BNNSs can be used to develop gas-sensor device. BNNSs-based gas-sensors can be potentially faster, and most important they can operate in harsh environment where properties of other material fall short.

Acknowledgements

This work is partially supported by NSF. We would like to thank Dr. Maxime Guinel and his staff for the assistance of TEM measurements.

References

[1] E. Massera, V.L. Ferrara, M. Miglietta, T. Polichetti, I. Nasti, G.D. Francia, Chem. Today (Chim. Oggi), 29 (2011) 39–41.
[2] H. Zeng, C. Zhi, Z. Zhang, X. Wei, X. Wang, W. Guo, Y. Bando, D. Golberg, Nano Lett. 10 (2010) 5049–5055.
[3] D. Pacile, J.C. Mayer, C.O. Girit, A. Zettl, Appl. Phys. Lett. 92 (2008) 133107–133109.
[4] Y. Lin, T.V. William, J.W. Connel, J. Phys. Chem. Lett. 1 (2010) 277–283.
[5] W. Qian, R. Hao, Y. Hou, Y. Tian, C. Shen, H. Gao, X. Liang, Nano Res. 2 (2009) 706–712.
[6] C.Z. Hu, F. Li, X.D. Liu, Acta Chim. Sinica 66 (2008) 1641–1646.
[7] L. Wang, C. Sun, L. Xu, Y. Qian, Catal. Sci. Technol. 1 (2011) 1119–1123.
[8] A. Rubio, J.L. Corkill, M.L. Cohen, Phys. Rev. B 49 (1994) 5081–5084.
[9] N.G. Chopra, R.J. Luyken, K. Cherrey, V.H. Crespi, M.L. Cohen, S.G. Louie, A. Zettl, Science 269 (1995) 966–967.
[10] D. Golberg, Y. Bando, M. Eremets, K. Takemura, K. Kurashima, H. Yusa, Appl. Phys. Lett. 69 (1996) 2045–2047.
[11] I. Mohai, M. Mohai, I. Bertoti, Z. Sebestyen, P. Nemeth, I.Z. Babievskaya, J. Szepvolgyew, Diamond Relat. Mater. 20 (2010) 227–231.
[12] M. Sajjad, P.X. Feng, Appl. Phys. Lett. 99 (2011), 253109-1–253109-4.
[13] X.P. Feng, H.X. Zhang, X.Y. Peng, M. Sajjad, J. Chu, Rev. Sci. Instrum. 82 (2011), 043303-1–043303-4.
[14] X.Y. Peng, M. Sajjad, J. Chu, B.Q. Yang, P.X. Feng, Appl. Surf. Sci. 257 (2011) 4795–4800.
[15] A. Zobelli, A. Gloter, C.P. Ewels, G. Seifert, C. Colliex, Phys. Rev. B 75 (2007) 245402.
[16] Z. Mingyao, W. Jianjun, C.H. Brian, R.A. Outlaw, Z. Xin, H. Kun, V. Shutthanandan, M.M. Dennis, Carbon 45 (2007) 2229–2234.
[17] R.J. Nemanich, S.A. Solin, R.M. Martin, Phys. Rev. B 23 (1981) 6348–6352.
[18] W.J. Zhang, S. Matsumoto, Chem. Phys. Lett. 330 (2000) 243–248.
[19] O.M. Moon, B.C. Kang, S.B. Lee, J.H. Boo, Thin Solid Films 464 (2004) 164–169.